Proceedings of the 1st Pacific International Conference on Application of Lasers and Optics 2004
<Edited by Milan Brandt and Erol Harvey>

CORRELATION BETWEEN MELT POOL TEMPERATURE AND CLAD FORMATION IN PULSED AND CONTINUOUS WAVE ND:YAG LASER CLADDING OF STELLITE 6

Shoujin Sun, Yvonne Durandet, Milan Brandt

Industrial Laser Applications Laboratory, Industrial Research Institute Swinburne
Swinburne University of Technology, Hawthorn, Vic, 3122, Australia

Abstract

The melt pool temperature in pulsed laser cladding of stellite 6 was measured with a two-colour pyrometer. The pulse peak temperature (T_p), durations when the melt pool temperature is above the melting points of stellite 6 powder (t_1) and substrate (t_2) in each pulse have been calculated and the effects of laser operating parameters (pulse energy, pulse frequency and spot overlap) on these values have been examined.

It is found that T_p only depends on the pulse energy and determines the melt pool size (D_M), whereas the ratios of both t_1 and t_2 to the pulse length increase with pulse energy, pulse frequency (f) and spot overlap. The predictions of clad height, the total thickness of clad layer and dilution by T_p, t_1 and t_2 are given for both pulsed and continuous wave (CW) laser cladding of stellite 6. Comparison between the experimental data and prediction has been made. Thick clad layer with low level of dilution requires higher value of the product of $t_1 \cdot f$, longer beam interaction time (τ) and large D_M.

Introduction

Laser cladding is a surfacing technique used to apply a metal coating onto a metal substrate to improve its wear, oxidation, erosion and corrosion resistances [1-3]. Its advantages include low heat input, low distortion of the workpiece and finer dendrite structure of the clad layer comparing with the conventional techniques such as PTA and TIG [4].

In some cases, it is required to produce a thick clad layer with minimum dilution to explore the maximum properties of the clad alloy such as the application of cobalt-based stellite alloy for improving the lifetime of low-pressure (LP) steam turbine blade [5, 6]. Therefore, the prediction and control of both clad height and dilution are demanded to meet the industrial requirement.

There are many reports on the continuous wave (CW) laser cladding [1-9], where the control of clad height and dilution is achieved simply by operating at an appropriated level of laser power and changing the scan rate and powder mass flow rate.

However, there is little research published on the pulsed laser cladding, which is an effective way to reduce further the heat input into the substrate and refine the layer microstructure. It is however more difficult to control the clad height and dilution of the pulsed laser cladding because of the additional variables, such as pulse frequency, pulse duration and pulse energy [10].

This paper presents a general model based on the measurement of melt pool temperature to predict the clad height and dilution for both CW and pulsed laser cladding. The model analysis has been verified by the experimental results.

Experimental procedures

Single-track cladding experiments involving both CW and pulsed laser claddings of stellite 6 on the AISI 420 grade stainless steel have been carried out. The chemical composition (wt.%) of stellite 6 powder (particle size range 53 to 180μm) was 1.57 C, 28.7 Cr, 1.0 Si, 3.9 W, 0.4 Fe, 1.6 Ni, 0.3 Mn with the balance Co. The chemical composition (wt.%) of steel substrate (thickness 10mm) was 0.41 C 14.3 Cr 0.70 Si, 0.45 Mn and the balance of Fe.

The CW laser cladding was carried out at laser power of 1200, 1400, 1600, 1800 and 2000W respectively. The scan rate was set at 900, 1200 and 1500mm/min respectively at each level of laser power.

The pulsed laser cladding was carried out at the pulse frequency of 40 and 60Hz respectively, the pulse length (the duration when the laser power is switched on) was fixed at 8ms for both pulse frequencies. At each pulse frequency, the pulse energy was set at 25, 18 and 14J/pulse respectively. The scan rates were selected to represent the spot overlaps of 89 and 83%. Details on the pulsed laser cladding can be found in [10].

The laser spot size was 3.5mm and the powder mass flow rate was set at low level of 11.7g/min for both CW and pulsed laser claddings in order to examine the effect of laser operating parameters on the clad height and dilution.

During cladding, the melt pool temperature was measured by a two-color pyrometer which was set up coaxially with the laser beam. The spot size of pyrometer was 2mm, and the sampling rate was 1kHz.

Analysis

Clad height

A typical temperature profile of the melt pool within a pulse is shown in Figure 1. The temperature increases to the peak (T_p) before the laser power is switched off following which it rapidly cools down. T_m^s and T_m^p are the melting points of the substrate and powder respectively. t_1 and t_2 are the durations when the melt pool temperature is above the melting points of powder and substrate respectively.

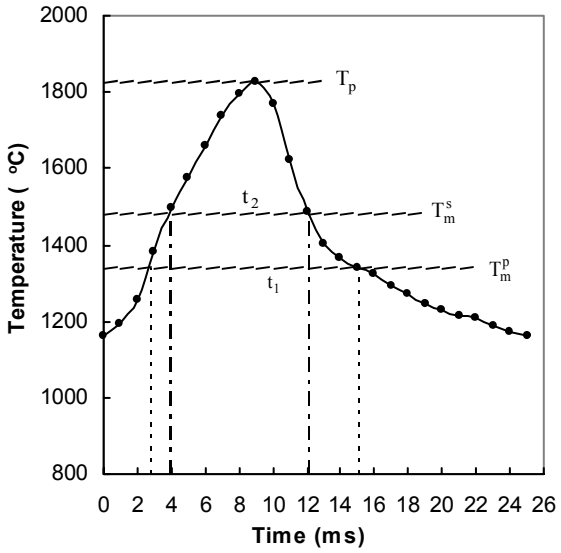

Figure 1. A typical melt pool temperature profile of pulsed laser cladding at pulse frequency of 40Hz. Data points reflect the sampling rate of 1kHz.

It is assumed that the powder injected into the melt pool is melted and deposited onto the surface of substrate only during the time the melt pool temperature is above the melting point of powder (i.e., within t_1). Therefore, the nominal clad height produced in one pulse is the volume of powder deposited on the substrate in one pulse divided by the clad area, i.e.:

$$h = \frac{\alpha \cdot t_1 \cdot \dot{m}}{\rho \cdot D_L^2} \qquad (1)$$

where, α is powder efficiency (the percentage of delivered powder melted in the melt pool), $\dot{m}$ is powder mass flow rate and ρ is the density of the alloy powder. Since the clad layer is the overlap of a number of pulses, and the number of overlapped pulses is $D_M \cdot f / v$, Therefore, the single-track clad height is:

$$H = \frac{h \cdot D_M \cdot f}{v} = \frac{\alpha \cdot \dot{m}}{D_L^2 \cdot \rho} \cdot f \cdot t_1 \cdot \tau \cdot \frac{D_M}{D_L} \qquad (2)$$

where, D_M is the melt pool diameter and $\tau = D_L / v$ is the laser beam interaction time, D_L is the laser spot size and v is the scan rate.

Thickness of clad and dilution

The clad thickness is the thickness of overall melted materials including the powder and substrate. The clad thickness in one pulse is dependent on the average temperature and the effective beam interaction time as follows:

$$T = K \cdot \left(T_i - T_m^s\right) \cdot \left(f \cdot t_2 \cdot \tau\right)^n + C \qquad (3)$$

where, K, n and C are the constants related to the thermal properties of the substrate and alloy powder, T_i is the average melt pool temperature within duration t_2 in a pulse.

The dilution is caused by the melting of substrate during cladding. It is calculated by:

$$D = \frac{T - H}{T} \times 100\% = \left(1 - \frac{H}{T}\right) \times 100\% \qquad (4)$$

Application of model analysis

Continuous wave laser cladding

The effects of laser power and scan rate on the clad height and total thickness of a single-track clad layer are shown in Figure 2. It can be seen that the clad height increases slightly with laser power, whereas the total thickness of clad layer increases dramatically with the laser power. Both the clad height and total thickness of clad layer increase with decreasing scan rate.

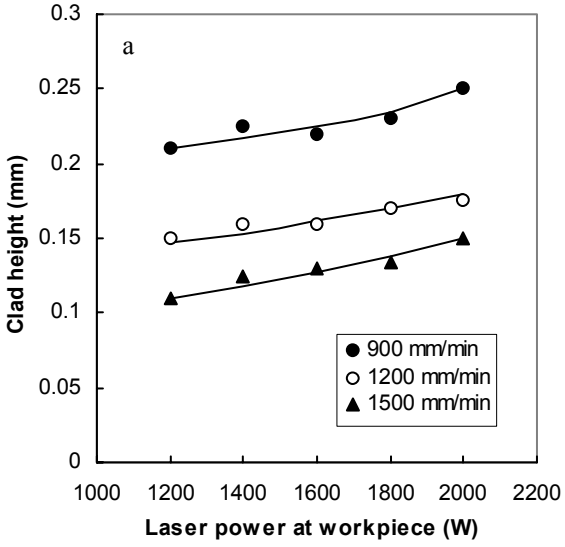

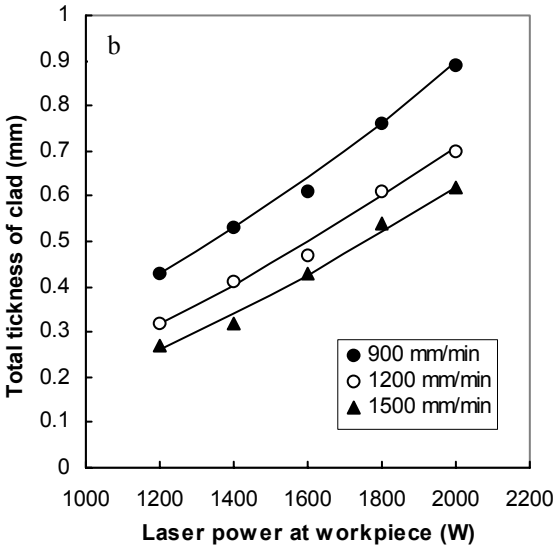

Figure 2. Effects of laser power and scan rate on (a) clad height and (b) total thickness of clad layer for continuous wave laser cladding

The effects of laser power and scan rate on the melt pool temperature are shown in Figure 3a. At the same powder mass flow rate, the melt pool temperature increases linearly with increasing laser power regardless of the scan rate. The melt pool size was measured from the transverse cross-section images of the single-track clad. The relationship between the melt pool size and melt pool temperature is shown in Figure 3b. Within the laser spot size and nozzle diameter, the melt pool size increases linearly with the melt pool temperature.

In the case of continuous wave laser, $f \cdot t_1 = 1$ and $f \cdot t_2 = 1$ therefore equations (2) and (3) can be simplified as:

$$H = \frac{\alpha \cdot \dot{m}}{D_L^2 \cdot \rho} \cdot \tau \cdot \frac{D_M}{D_L} \qquad (5)$$

$$T = K \cdot \left(T_i - T_m^s\right) \cdot \tau^n + C \qquad (6)$$

The comparisons between the measured and calculated clad height and total thickness of clad layer are shown in Figures 4 (a) and (b). The calculations were made using equations (5) and (6) for $\alpha = 50\%$, $\rho = 8.4 g/cm^3$, $D_L = 3.5mm$, $\dot{m} = 11.7 g/min$, $n = 1.3$, $C = 0.13mm$ and $K = 0.0135 mm/^oC/sec^{1.3}$. The values of the constants K, n and C are determined empirically.

The good agreements between the measured and calculated clad height and total thickness of clad layer indicate that the modeling analysis can predict the clad formation of CW laser cladding.

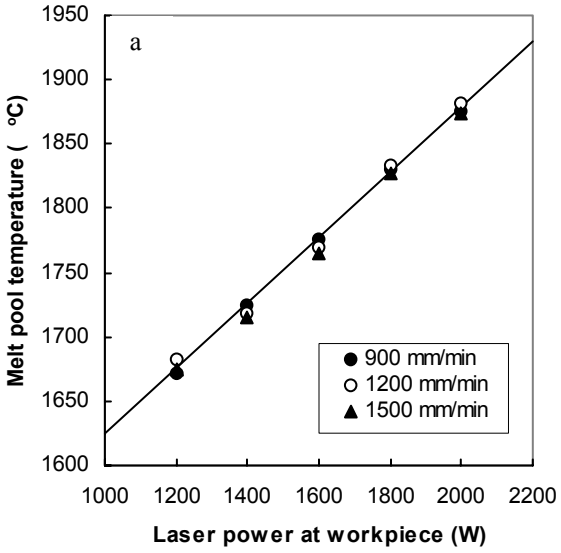

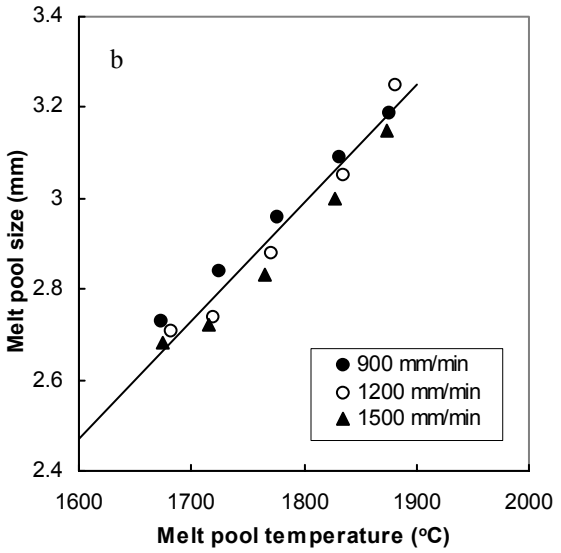

Figure 3. Relationships between (a) laser power and melt pool temperature, (b) melt pool temperature and melt pool size.

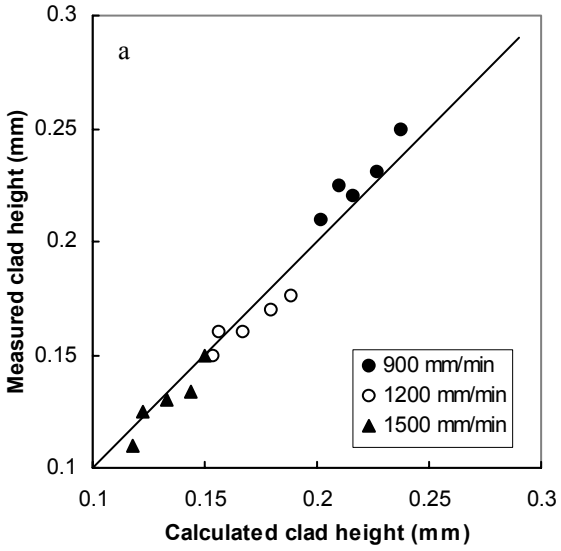

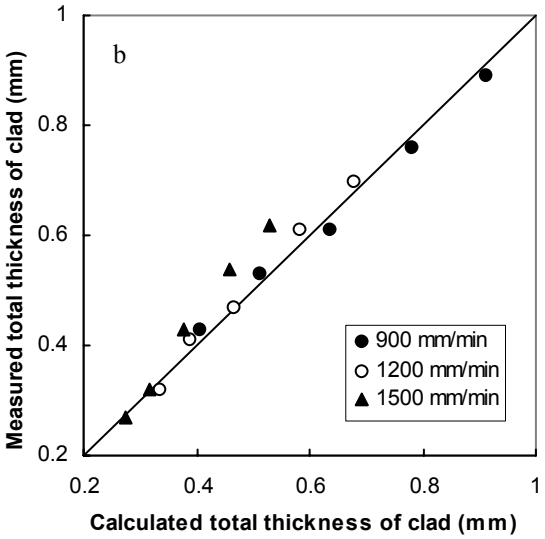

Figure 4. Correlation between the calculated and measured (a) clad height and (b) total thickness of clad layer for CW cladding.

Pulsed laser cladding

The experimental results of single-track pulsed laser cladding of stellite 6 are shown in Table 1. Both the clad height (H) and total thickness of clad layer (T) increase with pulse energy (E), pulse frequency (f) and spot overlap (SO). The effects of these parameters on the clad height are more severe than on the total thickness of clad layer.

Table 1 Results of single-track pulsed laser cladding

E (J/pulse)	f (Hz)	SO (%)	H (μm)	T (μm)	t_1 (ms)	t_2 (ms)
25	40	89	125.4	250.5	14.80	9.75
18	40	89	83.9	194.3	11.09	7.11
14	40	89	32.0	135.6	7.03	5.51
25	40	83	62.9	199.7	11.22	8.19
18	40	83	40.1	164.1	8.29	5.62
14	40	83	20.2	138.9	6.88	3.15
25	60	83	79.4	214.8	13.60	9.97
18	60	83	42.4	165.9	9.75	7.29
14	60	83	29.5	144.0	8.50	5.68

The averages of t_1 and t_2 calculated from all the pulses for the single-track cladding are also listed in Table 1. Despite the same pulse length (8 ms), the durations t_1 and t_2 in each pulse depend on the pulse energy, spot overlap and pulse frequency. The durations increase with pulse energy, pulse frequency and spot overlap because of the higher effect of the previous pulse, but the effect of pulse energy is more significant.

Regardless of pulse frequency and spot overlap, the peak temperature increases linearly with peak laser power as shown in Figure 5a. This is similar to continuous wave laser cladding, where the melt pool size is strictly dependent on the melt pool peak temperature (Figure 5b). The melt pool size increases linearly with melt pool peak temperature and reaches its maximum value, i.e. the laser spot size (3.5 mm) roughly at the melt pool temperature of 1950°C.

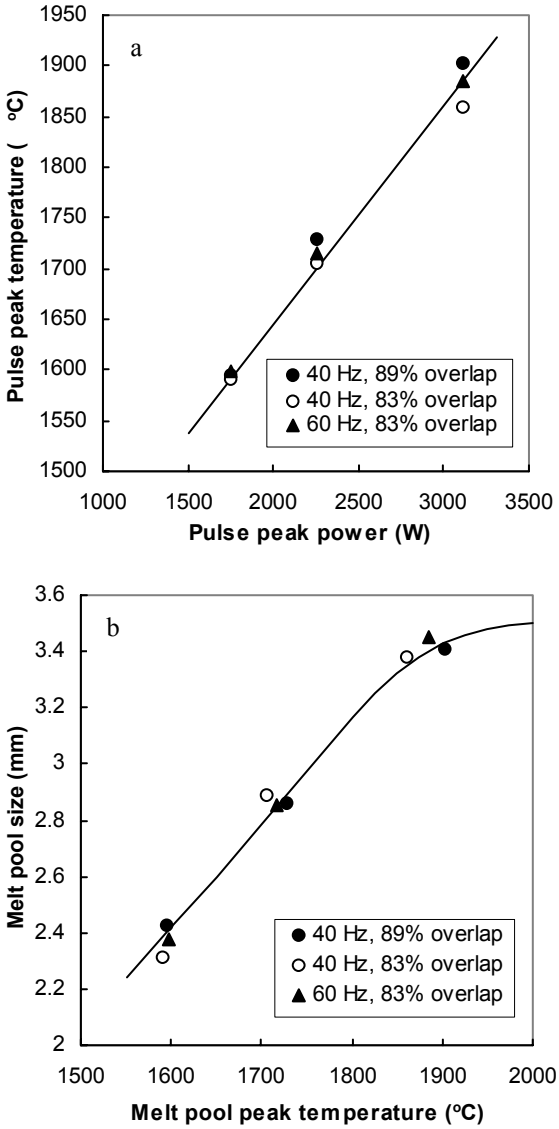

Figure 5. Relationships between (a) pulse peak power and pulse peak temperature and (b) pulse peak temperature and melt pool size.

Comparing Figures 3b and 5b, it can be found that the relationship between the melt pool size (in mm) and melt pool temperature (in °C) can be roughly described by:

$$D_M = 0.0036 \times T_p - 3.5 \text{ when } T_p \le 1950^\circ C \quad (7)$$

$$D_M = 3.5 \text{ when } T_p > 1950^\circ C \quad (8)$$

The correlation between the measured and calculated clad height and total thickness of clad layer for the pulsed laser cladding is shown in Figure 6. The calculations were made using equations (2) and (3) at the same values of the constants as those for the CW laser cladding. It is clear that the model can also predict the clad height and total thickness of clad layer for the pulsed laser cladding.

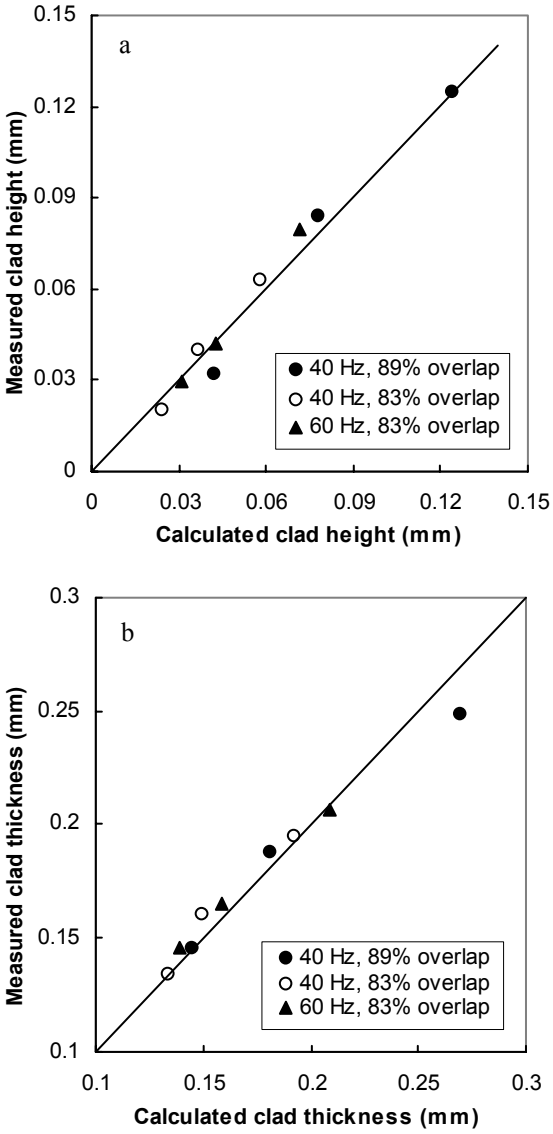

Figure 6. Comparison of the measured and calculated (a) clad height and (b) total thickness of clad layer for the single-track pulsed laser cladding.

Comparison between CW and pulsed laser cladding

There are many ways to compare the CW and pulsed laser cladding, such as based on the same laser power at the workpiece, or the same peak power. In this paper, comparisons have been made based on the (pulse peak) melt pool temperature as shown in Figure 7 and on the average laser power as shown in Figure 8. The solid lines are drawn based on the prediction from equations (2) and (3) for pulsed laser cladding (PLC) and equations (5) and (6) for CW laser cladding (CWLC). The symbols are obtained from experimental measurement. In this experiment, the powder mass flow rate was 11.7g/min, the scan rate was 900mm/min, and the pulse frequency for PLC was set at 40Hz.

Both the clad height and total thickness of clad layer of pulsed laser cladding are smaller than those of CW laser cladding at the same melt pool temperature because of the effects of the product of $t_1 \cdot f$ and $t_2 \cdot f$ as shown in equations (2) and (3), but the difference of total thickness is more significant. Since the product of $t_1 \cdot f$ increases with the melt pool temperature for the pulsed laser cladding, the difference of clad height between PLC and CWLC is smaller with increasing melt pool temperature.

The variation of dilutions with melt pool temperature shows totally different trend for PLC and CWLC as shown in Figure 7b. The dilution of CWLC increases with melt pool temperature but that of PLC decreases with increasing melt pool temperature which is attributed to the faster increase of clad height with melt pool temperature.

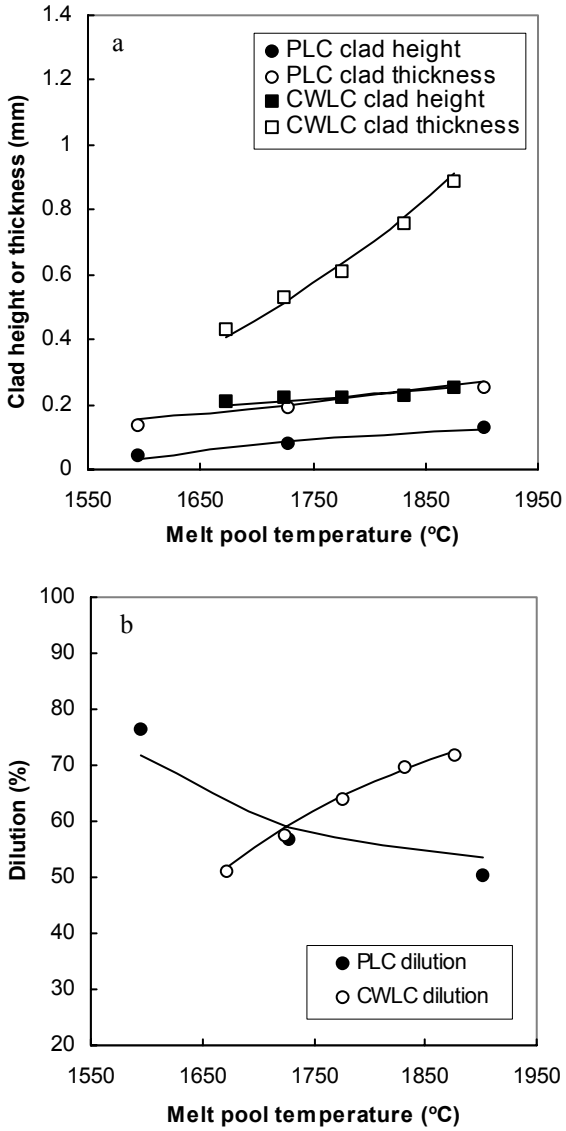

Figure 7. Comparison of (a) clad height and total thickness of clad layer and (b) dilution between pulsed and CW laser cladding on the melt pool temperature.

One advantage of pulsed laser cladding is that it can be done at very low average laser power (Figure 8) at which a good bonding clad layer can not be produced by CW laser. The ratio of clad height between PLC and CWLC

at same laser power is smaller than the product of $t_1 \cdot f$ due to the larger melt pool size of pulsed laser cladding. The dilution of pulsed laser cladding is lower at higher laser power whereas that of CW laser cladding is lower at lower laser power.

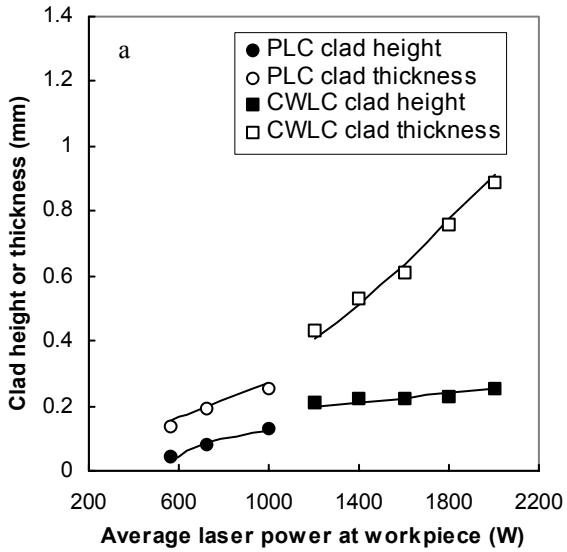

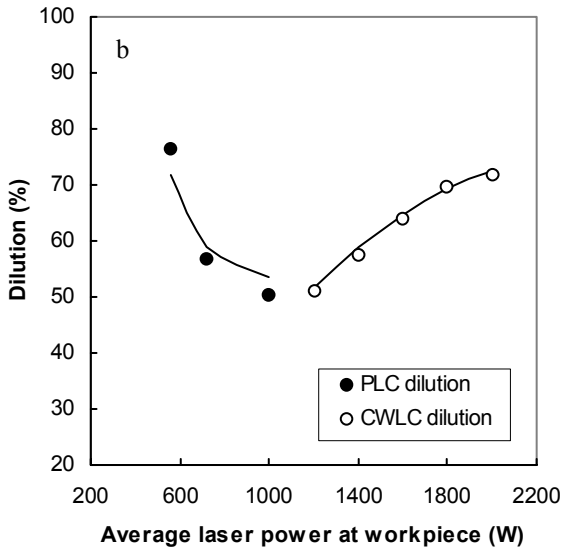

Figure 8. Comparison of (a) clad height and total thickness of clad layer and (b) dilution between pulsed and CW laser cladding as a function of the laser power at workpiece.

Conclusion

The model developed based on the melt pool temperature measurement in the present study can predict the stellite 6 clad formation and characteristics in both pulsed and continuous wave laser cladding.

In the case of CW laser cladding, the clad height increases slightly but the total thickness of clad layer increases dramatically with melt pool temperature. Therefore, the melt pool temperature must be strictly controlled to control the dilution.

For pulsed laser cladding, the durations when the melt pool temperature is above the melting points of stellite 6 powder (t_1) and substrate (t_2) in each pulse play important roles for clad height and total thickness in addition to the pulse peak temperature of the melt pool.

Dilution of CW laser cladding increases with melt pool temperature (or laser power) whereas the dilution of pulsed laser cladding decreases with melt pool temperature (or laser power) at the investigated range of laser power.

The higher value of the product of $t_1 \cdot f$, longer beam interaction time (τ) and large ratio of melt pool size against laser spot size (D_M / D_L) are required to produce thick clad layer with low level of dilution for pulsed laser cladding.

References

[1] Colaco R., Carvalho T. and Vilar R. (1994) Laser cladding of stellite 6 on steel substrate, High Temp. Chem. Processes 3, 21-29.

[2] So H., Chen C. T. and Chen Y. A. (1996) Wear behaviors of laser-clad stellite alloy 6, Wear 192, 78-84.

[3] De Hosson J. T. M. and De Mol van Otterloo L. (1997) Surface engineering with lasers: application to Co based materials, Surface Engineering 13, 471-481.

[4] Kathuria, Y. P. (2000) Some aspects of laser surface cladding in the turbine industry, Surface and Coatings Technology 132, 262-269.

[5] Peters T. and Jahnen W. 2002. Steam turbine leading edge repair by stellite laser cladding, Proceedings of EPRI, ST7.

[6] Shepeleva L., Medres B., Kaplan W. D., Bamberger M. and Weisheit A. (2000) Laser cladding of turbine blade, Surface and Coatings Technology 125, 45-48.

[7] Frenk A., Vandyoussefi M., Wagniere J.-D., Zryd A. and Kurz W. (1997) Analysis of the laser-cladding process for stellite on steel, Metallurgical and Materials Transactions 28B, 501-508.

[8] Steen W. M., Weerasinghe V. M. and Monson P. (1986) Some aspects of formation of laser clad tracks, in Proceedings of SPIE Vol. 650: High power laser and their industrial applications, 226-234.

[9] Weerasinghe V. M. and Steen W. M. (1987) Laser cladding with blown powder, Metal construction 19, 581-585.

[10] Sun S., Durandet Y. and Brandt M. (2003) Pulsed laser cladding of stellite 6 on stainless steel, in Proceedings of WTIA Surface Engineering Conference, Sydney, Australia.